Cyclic In-Plane Electron Delocalization (σ-Bishomoaromaticity) in 4N/5e Radical Anions and 4N/6e Dianions—Generation, Structures, Properties, Ion-Pairing, and Calculations

Kai Exner,*,† Oliver Cullmann,† Markus Vögtle,† Horst Prinzbach,*,† Birgit Grossmann,‡ Jürgen Heinze,‡ Lorenz Liesum,§ Rainer Bachmann,§ Arthur Schweiger,§ and Georg Gescheidt*,⊥

Contribution from the Institute of Organic Chemistry and Biochemistry and the Institute of Physical Chemistry, University of Freiburg, Albertstrasse 21, D-79104 Freiburg, Germany, Institute of Physical Chemistry, ETH Zürich, ETH Zentrum, CH-8000 Zürich, Switzerland, and Institute of Physical Chemistry, University of Basel, Klingelbergstrasse 80, CH-4056 Basel, Switzerland

Received April 28, 2000

Abstract: Cyclic delocalization of five and six electrons, respectively, in the plane of four N centers was explored by one-/two-electron reduction of more or less rigid, parallel bisdiazenes (**1**−**7**), with N═N/N═N distances ($d_{\pi\pi}$) ranging from ∼2.8 to 5.0 Å, interorbital angles (p,p; ω) from ∼l75° to 90°, and with more or less kinetic protection. For the "proximate" substrates **1**−**5** ($d_{\pi\pi} \approx 2.8-3.2$ Å, $\omega \approx 175-156°$), short contact with alkali metals (Li, Na, K, Cs) generates turquoise to deeply green radical anions (λ_{max}(DME) ≈ 700−900 nm). The character of these radical anions as cyclically in-plane delocalized bishomoconjugated 4N/5e species with a high concentration of spin density between the N═N units is established by extensive UV/vis, electrochemical, and EPR measurements (CW, pulsed) at temperatures down to 8 K, and by DFT calculations (B3LYP/6-31G*). After longer exposure to the metals, the three most persistent 4N/5e radical anions ($M^+\mathbf{1}^{\bullet-}$, $M^+\mathbf{2}^{\bullet-}$, $M^+\mathbf{5}^{\bullet-}$) are further reduced to the red dianions (**(**$2M^+\mathbf{1}^{2-}$, $2M^+\mathbf{2}^{2-}$, $2M^+\mathbf{5}^{2-}$, λ_{max}(THF) ≈ 360−430 nm). Of the nine ion pair combinations with Li^+, Na^+, and K^+ all except one ($2K^+\mathbf{1}^{2-}$) are thermally highly persistent. For the dianions the ^{1}H, ^{13}C, and ^{7}Li NMR analyses assisted by DFT calculations confirm the 4N/6e σ-bishomoaromatic electronic structure. The reduction potentials determined (CV) for dialkyl-diazenes (**8**−**10**) and bisdiazenes (**1**, **2**, and **5**) allow an estimate of the thermodynamic stabilization of the respective radical anions and of the gain in electron delocalization energy in the dianions (σ-bishomoaromaticity).

Introduction

Cyclic in-plane conjugation ("σ-aromaticity")—stabilization through cyclic electron delocalization in the plane of the ring-forming atoms[1,2]—denotes an intriguing concept in the theory of chemical bonding. This phenomenon, when brought about by σ-bishomoconjugation ($p_\sigma-p_\sigma$ orbital overlap), illustrated in Figure 1 for four-center systems, basically an extension of the classical π- and the well-established nonclassical π-homoaromaticity, is a rarity in that its operation is intrinsically bound to even tighter geometrical prerequisites. Experimentally, efficient cyclic in-plane delocalization has been verified in 4C/3e radical cations and σ-bishomoaromatic 4C/2e dications **A** (Figure 2) through one- and two-electron oxidation (superacid,[3] PE,[4] CV,[5] EPR[6]) of the polycyclic pagodanes (**C′**) and the respective "pagodadienes" (**D′**), with a peralkylated cyclobutane ring (**C**) and two proximate, *syn*-periplanar C═C double bonds (**D**), respectively, as rigidly preoriented four-carbon cores. In subsequent efforts to distinguish "tight" and "extended" (4C/

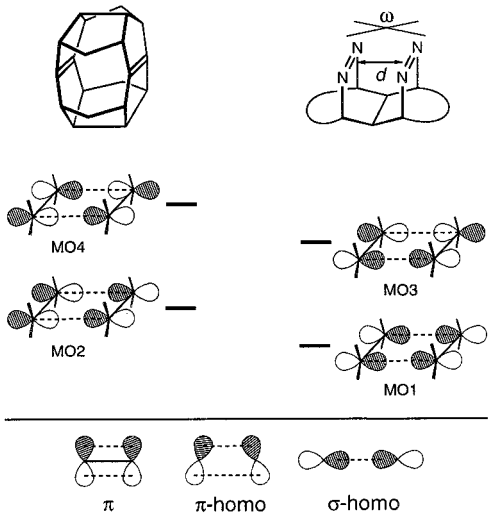

Figure 1. σ-Bishomoconjugation in homoconjugate cage dienes and corseted bisdiazenes. σ-Bishomoaromaticity is associated with the delocalization of two (dications) and four electrons (dianions). Extension of the classical π- to π-homo- to σ-homoconjugation.

† Institute of Organic Chemistry and Biochemistry, University of Freiburg.
‡ Institute of Physical Chemistry, University of Freiburg.
§ Institute of Physical Chemistry, ETH Zürich.
⊥ Institute of Physical Chemistry, University of Basel.

(1) Dewar, M. S. *J. Am. Chem. Soc.* **1984**, *106*, 669.
(2) (a) Homoconjugation in carbanions: Paquette, L. A. *Angew. Chem., Int. Ed. Engl.* **1978**, *17*, 106. (b) Stevenson, G. R. In *Molecular Structure and Energetics*; Liebman, J. F., Greenberg, A., Eds.; VCH: New York, 1986; p 57. (c) Haddon, R. C. *Acc. Chem. Res.* **1988**, *21*, 243. (d) *Aromaticity and Antiaromaticity*; Minkin, V. I., Glukhovtsev, M. N., Simkin B. Y., Eds.; Wiley: New York, 1994; Chapter 9. (e) Schleyer, P. v. R.; Jiao, H. *Pure Appl. Chem.* **1996**, *68*, 209−218. (f) For "aromaticity" in six-membered inorganic rings, see: Schleyer, P. v. R.; van Eikema Hommes, N. J. R.; Malkin, V. G.; Malkina, O. L. *J. Am. Chem. Soc.* **1997**, *119*, 12669.

10.1021/ja0014943 CCC: $19.00
Published on Web 10/14/2000

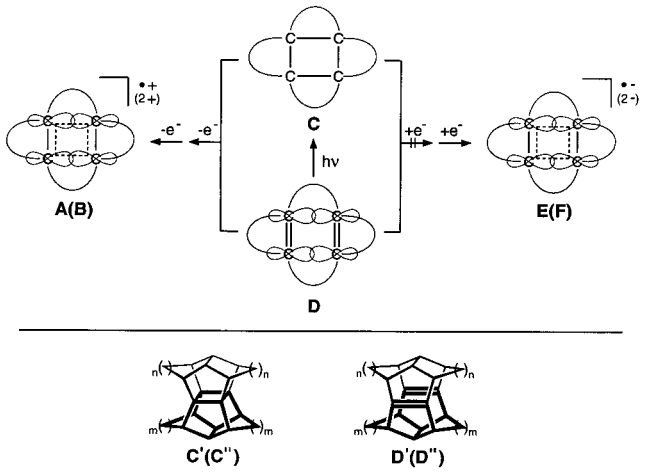

Figure 2. In-plane cyclically delocalized 4C/3e radical cations **A** and 4C/2e dications **B**, 4C/5e radical anions **E**, and 4C/6e dianions **F** derived from corseted cyclobutanes **C** and dienes **D**. Pagodanes **C′**, pagodadienes **D′**, and their "molecular halves" **C″** and **D″**.

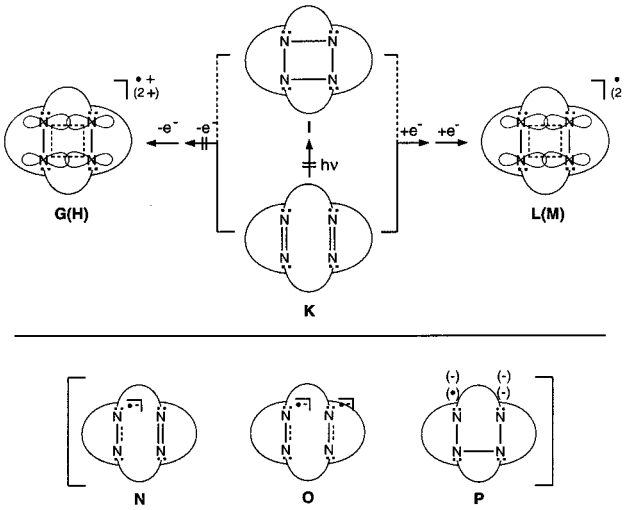

Figure 3. In-plane cyclically delocalized 4N/3e radical cations **G** and 4N/2e dications **H**, 4N/5e radical anions **L**, and 4N/6e dianions **M** derived from corseted tetraazetidines **I** and bisdiazenes **K**; alternative, localized structures **N**−**P**.

3e) precursor radical cations **A**[7] and to define "scope and limitations" of this sort of in-plane electron delocalization, in 1,16-dodecahedradiene at a π,π distance of ~3.5 Å ($\omega = 180°$),[6] still the 4C/3e radical cation, but not, however, the corresponding 4C/2e dication, could be detected.[8,9] The importance of "kinetic protection" is underlined by the failure to observe the dications derived from the less rigid "bird-cages" and their dienes (**C″**, **D″**).[3] Of particular relevance in the context of this paper is the fact that all these substrates (**C**, **D**) proved not amenable to reduction to give the respective (σ-bishomoaromatic) 4C/5(6)e (di)anions (**E**, **F**), not even after the installation of charge-stabilizing electronegative functionalities.

Given the higher electronegativity of nitrogen, these missing anionic bishomoconjugative bonding motifs should have a better chance in the form of 4N/5(6)e (di)anions (**L**, **M**, Figure 3): five (six) electrons are delocalized in the plane made up of four nitrogen centers and approached by one-/two-electron transfer to peralkylated, rigidly corseted tetraazetidines **I** or very proximate, near to *syn*-periplanar bisdiazenes **K**. It is understood that, given the exceptional concentration of 13 (14) n/p electrons in such 4N rings, anions of type **L** (**M**) would become observable only as pairs with appropriate counterions and in substrates which provide efficient kinetic protection (e.g., against diazene → hydrazone tautomerization). Bisdiazenes of this sort had been constructed with the—ultimately unsuccessful—intention to open photochemical access to so far unknown tetraazetidines.[10] An early oxidation study with the most "proximate" members (e.g., **2** in Figure 5) had not led to 4N/3e(2e) (di)cations **G** (**H**) but rather to standard[11] σ-type radical cations with practically no interaction between the neighboring N═N units.[12]

In this paper,[13,14] we present generation and characterization of 4N/5e radical anions **L** and 4N/6e σ-bishomoaromatic dianions **M** and specifically address the implicit questions: (i) Are the delocalized structures **L**/**M** distinguishable from localized (**N**/**O**, singlet/triplet) or tetraazane-type (**P**) configurations with potentially fast electron exchange? (ii) What is the influence of ion-pairing phenomena, of counterions, and of solvents upon electronic structure and stability?[15,16] (iii) What are the limiting geometrical prerequisites for cyclic electron delocalization, and what is the energetic gain? To find answers, we resorted to in

(3) (a) Prakash, G. K. S.; Krishnamurthy, V. V.; Herges, R.; Bau, R.; Yuan, H.; Olah, G. A.; Fessner, W.-D.; Prinzbach, H. *J. Am. Chem. Soc.* **1986**, *108*, 836. (b) Prakash, G. K. S. Krishnamurthy, V. V.; Herges, R.; Bau, R.; Yuan, H.; Olah, G. A.; Fessner, W.-D.; Prinzbach, H. *J. Am. Chem. Soc.* **1988**, *110*, 7764. (c) Herges, R.; Schleyer, P. v. R.; Schindler, M.; Fessner, W.-D. *J. Am. Chem. Soc.* **1991**, *113*, 3649. (d) Prakash, G. K. S. In *Stable Carbocation Chemistry*; Prakash, G. K. S., Schleyer, P. v. R., Eds.; Wiley: New York, 1997; p 137. (e) Etzkorn, M.; Wahl, F.; Keller, M.; Prinzbach, H.; Barbosa, F.; Peron, V.; Gescheidt, G.; Heinze, J.; Herges, R. *J. Org. Chem.* **1998**, *63*, 6080−6082.

(4) Martin, H.-D.; Mayer, B.; Weber, K.; Prinzbach, H. *Liebigs Ann.* **1995**, 2019.

(5) Weber, K.; Lutz, G.; Knothe, L.; Mortensen, J.; Heinze, J.; Prinzbach, H. *J. Chem. Soc., Perkin Trans. 1* **1995**, 1991.

(6) (a) Prinzbach, H.; Wollenweber, M.; Herges, R.; Neumann, H.; Gescheidt, G.; Schmidlin, R. *J. Am. Chem. Soc.* **1995**, *117*, 1439. (b) Gescheidt, G.; Herges, R.; Neumann, H.; Heinze, J.; Wollenweber, M.; Etzkorn, M.; Prinzbach, H.; *Angew. Chem., Int. Ed. Engl.* **1995**, *34*, 1016. (c) Gescheidt, G.; Prinzbach, H.; Davies, A. G.; Herges, R. *Acta Chem. Scand.* **1997**, *51*, 174. (d) Prakash, G. K. S.; Weber, K.; Olah, G. A.; Prinzbach, H.; Wollenweber, M.; Etzkorn, M.; Voss, T.; Herges, R. *J. Chem. Soc., Chem. Commun.* **1999**, 1029.

(7) Trifunac, A.; Werst, D.; Herges, R.; Neumann, H.; Prinzbach, H.; Etzkorn, M. *J. Am. Chem. Soc.* **1996**, *118*, 9444.

(8) (a) Prinzbach, H.; Gescheidt, G.; Martin, H. D.; Herges, R.; Heinze, J.; Prakash, G. K. S.; Olah, G. A. *Pure Appl. Chem* **1995**, *67*, 673. (b) Weiler, A.; Quennet, E.; Exner, K.; Keller, M.; Prinzbach, H. *Tetrahedron Lett.* **2000**, *41*, 4763. (c) Reinbold, J. Dissertation, University of Freiburg, 2000.

(9) Weber, K.; Prinzbach, H.; Schmidlin, R.; Gerson, F.; Gescheidt, G. *Angew. Chem., Int. Ed. Engl.* **1993**, *32*, 875.

(10) Exner, K.; Fischer, G.; Bahr, N.; Beckmann, E.; Lugan, M.; Yang, F.; Rihs, G.; Keller, M.; Hunkler, D.; Knothe, L.; Prinzbach, H. *Eur. J. Org. Chem.* **2000**, 763 and references cited therein.

(11) Nelsen, S. F. In *The chemistry of the hydrazo, azo and azoxy groups*; Patai, S., Ed.; Wiley: New York, 1997; Chapter 6.

(12) (a) Prinzbach, H.; Fischer, G.; Rihs, G.; Sedelmeier, G.; Heilbronner, E.; Yang, Z.-z. *Tetrahedron Lett.* **1982**, 1251. See also: (b) Marterer, W.; Prinzbach, H.; Rihs, G.; Wirz, J.; Lecoultre, J.; Heilbronner, E. *Helv. Chim. Acta* **1988**, *71*, 1937.

(13) Exner, K. Dissertation, University of Freiburg, 1998.

(14) For a preliminary publication, see: Exner, K.; Hunkler, D.; Gescheidt, G.; Prinzbach, H. *Angew. Chem., Int. Ed. Engl.* **1998**, *37*, 1910. Very recently, π-bis(tris)homoaromatic 3B/2e dianions have been reported: Lösslein, W.; Pritzkow, H.; Schleyer, P. v. R.; Schmitz, R.; Siebert, W. *Angew. Chem., Int. Ed.* **2000**, *39*, 1276. Scheschkewitz, D.; Ghaffari, A.; Amseis, P.; Unverzagt, M.; Subramanian; G.; Hofmann, M.; Schleyer, P. v. R.; Schaefer, H. F., III; Geiseler, G.; Massa, W.; Berndt, A. *Angew. Chem., Int. Ed.* **2000**, *39*, 1272.

(15) (a) Bachmann, R.; Gerson, F.; Gescheidt, G.; Vogel, E. *J. Am. Chem. Soc.* **1993**, *115*, 10286. (b) Scholz, M.; Gescheidt, G.; Daub, J. *J. Chem. Soc., Chem. Commun.* **1995**, 803. (c) Scholz, M.; Gescheidt, G.; Schoeberl, U.; Daub, J. *J. Chem. Soc., Perkin Trans. 2* **1995**, 209.

(16) (a) Sharp, J. H.; Symons, C. R. In *Ions and Ion Pairs in Organic Reactions*; Szwarc, M., Ed.; Wiley: New York, 1972; Vol. 1, Chapter 5. (b) Staley, S. W.; Grimm, R. A.; Boman, P.; Eliasson, B. *J. Am. Chem. Soc.* **1999**, *121*, 7182 and references cited therein.

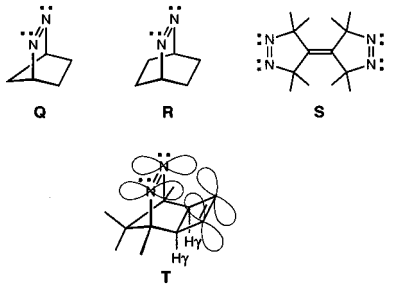

Figure 4. Diazene reference structures **Q**−**T**.

situ UV/vis, electrochemical (CV), CW and pulsed EPR/ENDOR, and NMR (^{1}H, ^{13}C, ^{7}Li) measurements and quantum chemical calculations.

Background

Electron transfer to *mono*diazenes has been intensively studied. Since diazenes carrying β-hydrogens are subject to base/acid-catalyzed tautomerization into normally more stable hydrazones, these studies (EPR,[17] CV[18]) have been preferably performed with diaryl- and dialkyl-diazenes, the latter being either β-alkylated or part of a polycyclic carbon skeleton with hardly removable β-hydrogens. From the EPR studies by Gerson et al.[19−21] and Gescheidt et al.,[22] the diazenes **Q**−**T** (Figure 4) are taken as reference structures. For the radical anions of the diazabicyclo[2.2.1]heptene (**Q**) and diazabicyclo[2.2.2]octene (**R**) type—the parent structural subunits of the two most prominent bisdiazenes in this paper (**1** and **2**, Figure 5)—concentration of most of the spin density in the π-region of the N═N group was established by ^{14}N hyperfine coupling constants (hfc's) of 0.8−0.9 mT. From harder to softer counterions, exercising different spin-transfer mechanisms (Li^+ negative, Na^+−Cs^+ positive hfc's), ion-pairing and hyperfine interactions with the metal become less pronounced. The radical anion of bisdiazene **S** stands for the localization of the unpaired electron on one of the two N═N units. The following statements are important for upcoming discussions in this paper: For the radical anion of diazene/ene **T**, a surprisingly large hyperfine coupling constant of the γ-protons ($a_{H\gamma}$ = 0.64 mT) was proposed as evidence for the π-homoconjugative N═N/C═C interaction. It has to be stressed that, in the EPR studies, for none of the many reduced dialkyl diazenes was any mention made of further reduction to the respective dianions.[19−22] Similarly, in the extensive literature on the electrochemistry of diazenes,[18] no example for the successful reduction of a dialkyl diazene is found (the one report had to be corrected[20]).

Substrates

The bisdiazenes of type **K** utilized in this study are listed in Figure 5; the details of their synthesis have been (**1**,[10] **2**,[10] **6**,[10] **7**[23]) or will be (**3**,[24] **4**, **5**) part of separate publications.[25] The skeletal substitution in **1**, **2**, and **6** was dictated by synthetic reasons, that in **5** was effected in order to enforce a shortening of the π,π distance and to prohibit diazene → hydrazone tautomerization. In this latter respect, the diazabicycloheptene (DBH, **Q**) and, somewhat less, diazabicyclooctene units (DBO, **R**) in **1** and **2** are known to provide effective "anti-Bredt-protection". Monodiazenes **8**, **9**, and **10**[10] serve as reference compounds (UV/vis, CV).

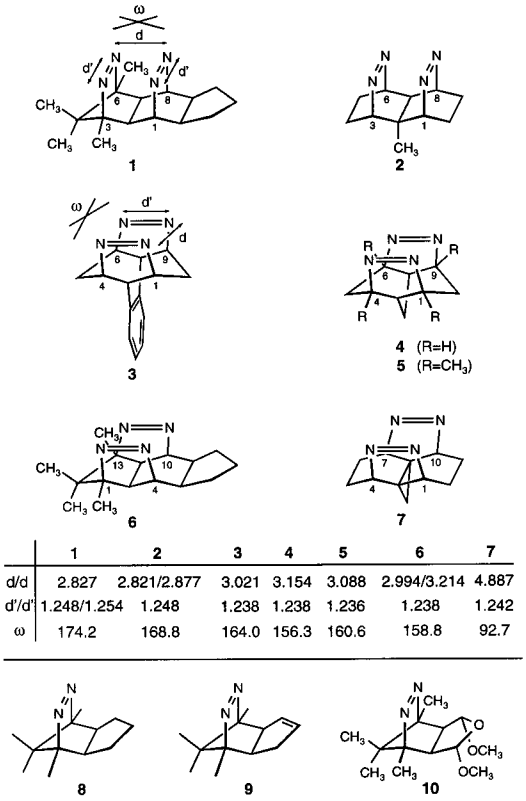

	1	2	3	4	5	6	7
d/d	2.827	2.821/2.877	3.021	3.154	3.088	2.994/3.214	4.887
d′/d′	1.248/1.254	1.248	1.238	1.238	1.236	1.238	1.242
ω	174.2	168.8	164.0	156.3	160.6	158.8	92.7

Figure 5. Pool of bisdiazenes **1**−**7**. Calculated (B3LYP/6-31G*) transanular N═N/N═N distances (d, Å), N═N bond lengths (d', Å), and interorbital angles (ω, deg). Monodiazenes **8**−**10** as references.

In the search for the most suitable method to make a reliable, consistent comparison of the substrate bisdiazenes with their 4N/5e radical anions and 4N/6e dianions, various computational methods have been checked against the crystallographic data available for several bisdiazenes; the B3LYP/6-31G* method[26] in every respect showed the best fits (cf. Table 3 in ref 10, Table 5 in the Supporting Information).[27] In Figure 5 for the bisdiazenes **1**−**7**, the B3LYP/6-31G*-calculated N═N bond lengths (d'), transanular N═N/N═N distances (d), and interorbital angles (ω, angle between the p-axes of the two facing diazene moieties; 180° for perfect in-plane orientation) are given. As judged by these "stereoelectronic" parameters, rigid **1** and

(17) Gerson, F. *Helv. Chim. Acta* **1992**, *75*, 335.
(18) Simonet, J.; Gueguen-Simonet, N. In *The chemistry of the hydrazo, azo and azoxy groups*; Patai, S., Ed.; Wiley: New York, 1997; Chapter 12.
(19) Ess, C. H.; Gerson, F.; Adam, W. *Helv. Chim. Acta* **1991**, *74*, 2078; **1992**, *75*, 335.
(20) (a) Gerson, F.; Sahin, C. *J. Chem. Soc., Perkin Trans. 2* **1997**, 1127. (b) For CV measurements of tetraalkyltetraazenes, see: (a) Nelsen, S. F.; Peacock, V. E.; Kessel, C. R. *J. Am. Chem. Soc.* **1978**, *100*, 7017. (b) Bock, H.; Göbel, I.; Näther, Ch.; Solouki, B.; John, A. *Chem. Ber.* **1994**, *127*, 2197.
(21) Gerson, F.; Lamprecht, A.; Scholz, M.; Troxler, H.; Lenoir, D. *Helv. Chim. Acta* **1996**, *79*, 307.
(22) (a) Gescheidt, G.; Lamprecht, A.; Rüchardt, C.; Schmittel, M. *Helv. Chim. Acta* **1992**, *75*, 351. Cf.: (b) Sustmann, R.; Sauer, R. *J. Chem. Soc., Chem. Commun*. **1985**, 1248. (c) Russell, G. A.; Konaka, R.; Strom, E. T.; Danen, W. C.; Chang, K.; Kaupp, G. *J. Am. Chem. Soc.* **1968**, *90*, 4646.
(23) Bahr, N.; Beckmann, E.; Mathauer, K.; Hunkler, D.; Keller, M.; Prinzbach, H.; Vahrenkamp, H. *Chem. Ber.* **1993**, *126*, 429−440.
(24) Cullmann, O. Dissertation, University of Freiburg, 1998. Cullmann, O.; Vögtle, M.; Stelzer, F.; Prinzbach, H. *Tetrahedron Lett.* **1998**, *38*, 2303.
(25) Beckmann, E.; Bahr, N.; Cullmann, O.; Yang, F.; Kegel, M.; Exner, K.; Knothe, L.; Prinzbach, H., in preparation.
(26) (a) Frisch, M. J.; Trucks, G. W.; Schlegel, H. B.; Gill, P. M. W.; Johnson, B. G.; Robb, M. A.; Cheeseman, J. R.; Keith, T.; Petersson, G. A.; Montgomery, J. A.; Raghavachari, K.; Al-Laham, M. A.; Zakrzewski, V. G.; Ortiz, J. V.; Foresman, J. B.; Cioslowski, J.; Stefanov, B. B.; Nanayakkara, A.; Challacombe, M.; Peng, C. Y.; Ayala, P. Y.; Chen, W.; Wong, M. W.; Andres, J. L.; Replogle, E. S.; Gomperts, R.; Martin, R. L.; Fox, D. J.; Binkley, J. S.; Defrees, D. J.; Baker, J.; Stewart, J. P.; Head-Gordon, M.; Gonzalez, C.; Pople, J. A. *Gaussian 94*, Revision E.2; Gaussian, Inc.: Pittsburgh, PA, 1995. (b) Becke, A. D. *J. Chem. Phys.* **1993**, *98*, 1372. (c) Lee, C.; Parr, R. G. *Phys. Chem. B* **1988**, *37*, 785.
(27) Wiest, O.; Houk, K. N. *Top. Curr. Chem.* **1996**, *183*, 2.

2 come closest to the caged dienes **D**, for which two-electron oxidation had led to persistent σ-bishomoaromatic dications **B**. In fact, in the case of **1** and **2** (but not of **6** and **7**), through-space (TS) interaction had been manifested by typical UV absorptions.[10] For **3**−**6** it has to be remarked that, with d = 3.0−3.2 Å and ω = 164−156° for their thermodynamically most stable conformation, they are not only less proximate but also, in contrast to the rigid skeletons **1** and **2**, rather flexible, and hence more apt to respond to the addition of electrons by geometrical changes. For the most "distant" **7**, a conformation "closed" to a 3.2-Å π,π distance (ω = 167.5°) is ∼20 kcal mol^{-1} higher in energy than the "open" one shown.

UV/Vis Spectroscopic Measurements

For the UV/vis (and EPR) measurements, solutions of the bisdiazene radical anion/counterion pairs were generated as described for the *mono*diazenes[19−22] in carefully deoxygenated anhydrous THF and DME as solvents, with Li wire or mirrors of Na, K, and Cs, respectively. Anions with Li^+ as counterion were also prepared by Li/K exchange. Simultaneous recording of the UV/vis and EPR spectra inside the microwave cavity of the EPR spectrometer guaranteed that measurements were made using the very same sample under identical conditions.[28]

Since for the reference dialkyl-diazene radical anions **Q**$^{\bullet-}$−**T**$^{\bullet-}$ no UV/vis absorptions were reported, the reduction **10** → **10**$^{\bullet-}$ served as a model case (K, DME, 298 K). The colorless THF solution became light yellow, and the longest-wavelength absorption (λ_{max} = 359 nm, n → π*) shifted bathochromically by ∼20 nm to 380 nm.

In visible contrast, short exposure (∼15 s) of bisdiazene **1** to Li, Na, K, or Cs produced a turquoise (Li) to brilliant green (Na, K, Cs) color. Upon longer contact, kinetically neatly controllable (up to 3−5 min for NMR samples), this color changed to red (golden-yellow in high dilution, Li, Na) or dirty brown (K, Cs). Green, metal-free solutions and solid samples of Li^+**1**$^{\bullet-}$ kept at room temperature did not change for months—upon their contact with air, instantaneous decoloration occurred, whereupon neutral **1** was quantitatively recovered. There is the expected influence of the counterion: the maxima of the broad, featureless longest-wavelength absorption bands (Table 1, half-band-width ∼220 nm) are shifted by as much as 108 nm from 712 nm for Li^+**1**$^{\bullet-}$ to 820 nm for Cs^+**1**$^{\bullet-}$, in line with a substantial weakening of the ion-pairing. The appearance of these bands is suggestive of a marked structural difference between the S_0 and S_1 states in the course of the electronic excitation (Figure 1, cf. the nodal structure of the orbitals MO3 and MO4, respectively), fluctuations in the position of the counterions may further contribute to the lack of any structural feature. For a given ion pair there is no significant solvent effect, and a measurable temperature effect is found only for Na^+**1**$^{\bullet-}$ (hypsochromic shift with increasing temperature caused by tighter ion-pairing due to the lower polarity of the solvent[16]).

The Li^+, Na^+, and K^+ ion pairs of **2**$^{\bullet-}$ (Table 1) exhibit an UV/vis absorption (color) very similar to that of the M^+**1**$^{\bullet-}$ pairs, similarly red-shifted with decreasing coordination abilities of the counterions, although the shift is less pronounced ($\Delta\lambda$ = 57 nm).

Bisdiazenes **3**, **4**, and **5** were reduced only with potassium. The longest-wavelength UV/vis absorption maxima of the deeply red K^+**3**$^{\bullet-}$, K^+**4**$^{\bullet-}$, and K^+**5**$^{\bullet-}$ solutions (DME, 298 K) are again more red-shifted by 20−80 nm with respect to K^+**1**$^{\bullet-}$. Thermally, the salts of **2**$^{\bullet-}$ and **5**$^{\bullet-}$, as solids or solutions, are persistent for days at room temperature, while K^+**3**$^{\bullet-}$ and K^+**4**$^{\bullet-}$ decay within minutes. Upon exposure of bisdiazenes **6** and **7** to K/DME (230−296 K), no color evolved—not surprisingly for "distant" **7**, and in the case of **6** presumably a consequence of even less kinetic stabilization of K^+**6**$^{\bullet-}$ than for K^+**3**$^{\bullet-}$ and K^+**4**$^{\bullet-}$.

(28) Gescheidt, G. *Rev. Sci. Instrum* **1994**, *65*, 2145.

Table 1. Dependence of the Longest-Wavelength UV/Vis Absorption Maxima of Radical Anions **1**$^{\bullet-}$−**5**$^{\bullet-}$ on Counterion, Solvent, and Temperature (**10**$^{\bullet-}$ as Reference)

	M^+	solvent	T (K)	λ_{max} (nm)
1$^{\bullet-}$	Li^+	THF	193−298	712
	Li^+	DME	273	709
	Li^+/LiCl	THF	202−303	753
	Na^+	THF	183−298	787−761
	K^+	DME	202−282	820
	K^+	THF	232−298	820
	Cs^+	THF	202−232	820
2$^{\bullet-}$	Li^+	THF	298	716
	Na^+	THF	213−298	744−733
	K^+	THF	213−298	764−768
	K^+	DME	233	773
3$^{\bullet-}$	K^+	DME	298	840
4$^{\bullet-}$	K^+	DME	298	881
5$^{\bullet-}$	K^+	DME	213−298	893−900
10$^{\bullet-}$	K^+	DME	298	380

Table 2. Dependence of the Longest-Wavelength UV/Vis Absorption Maxima of the Dianions **1**$^{2-}$, **2**$^{2-}$, and **5**$^{2-}$ on Counterion (THF, Room Temperature)

	$2Li^+$	$2Na^+$	$2K^{2+}$
1^{2-}	396	423	
2^{2-}	367	382	397
5^{2-}	373		

The radical anions of bisdiazenes **1**, **2**, and **5** were sufficiently persistent to allow their convenient and neat reduction to give golden-yellow (red) dianions through longer exposure to the metals (Li, Na, K). The red-shift of the longest-wavelength absorption maxima (Table 2) with increasing softness of the counterions turned out to be much smaller than that for the radical anions (Table 1). The spectra proved to be practically temperature invariant between 203 and 298 K. The exception was K^+**1**$^{\bullet-}$, for which the green color directly changed into a dirty brown. The UV/vis absorbance of the dianions remained constant for weeks at room temperature, and in the case of $2Li^+$**1**$^{2-}$ even for several months.

There is a lesson to be learned from this section: For the ion pairs M^+**1**$^{\bullet-}$−M^+**5**$^{\bullet-}$ ($2M^+$**1**$^{2-}$, $2M^+$**2**$^{2-}$, $2M^+$**5**$^{2-}$), the green (red) color caused by their UV/vis absorption between 700 and 900 (360−400) nm is visible evidence for effective electron delocalization. That for the M^+**1**$^{\bullet-}$ series the continuous red-shift of the generally very broad, unstructered absorption bands is not accompanied by a significant change in appearance speaks for the presence of radical anions with uniform electronic structures; not even strong ion-pairing enforces localization. The lifetime of these anions expectedly decreases sharply with decreasing N═N/N═N distances and increasing interorbital angles. Yet, as manifested by the pair **4**/**5**, the degree of kinetic protection offered by the respective molecular skeleton plays a crucial role, and $d_{\pi\pi} \approx$ 3.2 Å ($\omega \approx$ 155°) certainly does not mark the limit for homoconjugational interaction.

Electrochemical (CV) Measurements[29,30]

As stated in the Introduction, prior attempts to electrochemically reduce *dialkyl*-diazenes had been unsuccessful; the crux is an experimentally hardly accessible potential range more negative than −2.8 V.[20] On the other hand, the reduction of

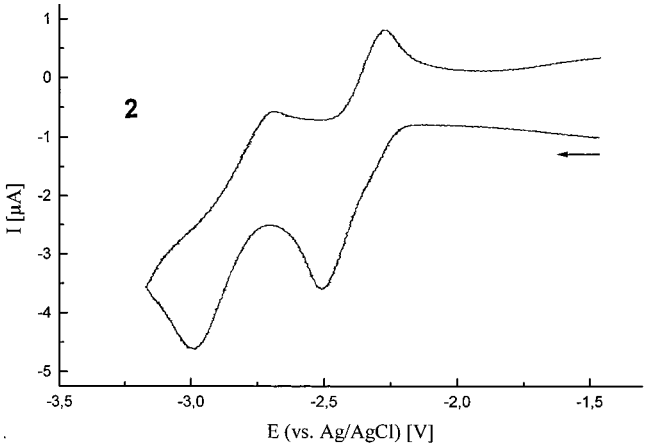

Figure 6. Cyclic voltammogram of **2** (THF/$TBAPF_6$ (0.1 N) 0.1 V s^{-1}, room temperature, vs Ag/AgCl).

Table 3. Reduction Potentials (V) of Bisdiazenes **1**, **2**, and **5** and Monodiazenes **8**−**10** (THF/0.1 M $TBAPF_6$, 0.1 V s^{-1}, Room Temperature) and Calculated Relative Electron Affinities (EA [eV], B3LYP/6-31G*)

	reduction 1	reduction 2	rel. EA
1	$E_{1/2} = -2.38$ V	$E_{pc} = -2.90$ V	0.0
2	$E_{pc} = -2.45$ V	$E_{pc} = -2.87$ V	0.08
	$E_{1/2} = -2.36$ V[a]		
5	$E_{1/2} = -2.72$ V		0.33
8	$E_{pc} = -3.10$ V		
	$E_{1/2} = -2.90$ V[a]		
9	$E_{pc} = -3.00$ V		
	$E_{1/2} = -2.70$ V[a]		
10	$E_{pc} = -2.77$ V		
	$E_{1/2} = -2.74$ V[b]		

[a] 0.1 V s^{-1}, −30 °C. [b] 1 V s^{-1}, room temperature.

diaryl-diazenes offering efficient charge delocalization was unproblematic; e.g., for diphenyl-diazene (azobenzene) in CH_3CN(TBABF$_4$, Ag/$AgNO_3$ (0.1 N), 22 °C, 0.2 V s^{-1}), the reversible one-electron reduction occurs at −1.72 V, followed by a not completely reversible second reduction at −2.4 V.[18,31] Hence, the expectation was justified that efficient in-plane delocalization as formulated with bisdiazene radical anions **L** should shift the first and even the second reduction potential of the proximate bisdiazenes **1**−**6** into an experimentally accessible range.

Indeed, with the very carefully dried solvent/electrolyte system THF/$TBAPF_6$ (0.1 N), the redox behavior of bisdiazenes **1**, **2**, and **5** (selected for the persistence of the derived radical anions) and even of the monodiazenes **8**−**10** could be unraveled (Figure 6, Table 3). For the latter three, representing the diazabicyclo[2.2.1]heptene unit of **1** and **2**, after some experimentation, reversible reduction potentials in the predicted range of −2.9 to −2.7 V were measured. For the most proximate, best aligned, and rigid **1** ($d_{\pi\pi}$ = 2.83 Å, ω = 174.2°) and **2** ($d_{\pi\pi}$(av) = 2.85 Å, ω = 168.8°, Figure 5), not only was the first potential significantly lowered ($E_{1/2}$ = −2.38 and −2.36 V, respectively), but was also followed by a not fully reversible second reduction wave (−2.90 and −2.87 V, respectively). In the case of **5** ($d_{\pi\pi}$ = 3.1 Å, ω = 160.6°), the reversible wave with $E_{1/2}$ = −2.72 V was significantly more negative (in fact, hardly different from that of the monodiazenes **9**/**10**); up to the experimental limits (ca. −3.2 V), no second reduction wave was recorded.

In brief, with $E_{1/2} \approx -2.7$ V (**10**) as reference value for a localized radical anion of type **N** (Figure 3)—the inductive effect of the second N═N unit in **1** and **2** being set equal to that of the acetal unit in **10**, and with differential effects in ion association and solvation for mono- and dianions being neglected—the difference of $\Delta E \approx 0.3$ V for the first reduction of **1** and **2** becomes a thermodynamically meaningful measure of the delocalization energy gained by the radical anions $\mathbf{1}^{\bullet-}$ and $\mathbf{2}^{\bullet-}$, which is counterbalanced primarily by the energy needed for the moderate (but in the rigid skeletons nevertheless rather costly) structural changes involved. That the second potentials are more negative by only ∼0.5 V is taken as evidence that, in the dianions, Coulombic effects due to the excessive charge concentration are in good part offset by the gain in cyclic delocalization energy. The failure to observe a second reduction wave for **5** reflects the significantly more negative potential for the first reduction (lower electron affinity) and can be safely ascribed to the less favorable stereoelectronic situation since differences in strain between the pyrazolidine rings in **5** and **1**/**2** should have no significant impact on the N═N reduction potentials.[29] The energetic costs of ∼0.5 V for the reductions $\mathbf{1}^{\bullet-} \rightarrow \mathbf{1}^{2-}$ and $\mathbf{2}^{\bullet-} \rightarrow \mathbf{2}^{2-}$—compare ΔE = 0.7 V for the above-cited first and second reductions of azobenzene—seem high when compared with the 0.2−0.25 V reported for the reduction of the (homo)cyclooctatetraene radical anions to the (homo)-aromatic dianions; clearly, in these larger annulene dianions, the electron−electron repulsion is much weaker.[1a−c,32] The relative electron affinities calculated for **1**, **2**, and **5** (Table 3) parallel the measured reduction potentials.[33,34]

EPR Spectroscopic Measurements and Calculations

For the most proximate bisdiazene **1**, the EPR spectra obtained after one-electron reduction with Li, Na, K, and Cs are displayed in Figure 7. As in case of the UV/vis spectra, the temperature response of the EPR signals can be taken as indicative of ion-pairing phenomena: whereas the low-temperature spectrum of $Li^+\mathbf{1}^{\bullet-}$ is an unresolved line, a slight resolution becomes discernible at higher temperatures. A parallel behavior holds for the Li^+(LiCl) spectra; this is in line with a negative sign of the ^{7}Li hfc, where the absolute value decreases at elevated temperatures and thus contributes decreasingly to the EPR line width. The $Na^+\mathbf{1}^{\bullet-}$ spectra consisting of 13 distinct lines are inversely temperature dependent, pointing to a positive ^{23}Na hfc; its absolute value increases with temperature. The

(29) Very recently for diazabicyclo[2.2.2]octene, an irreversible reduction potential of −2.8 V (vs SCE, acetonitrile) was published: Pischel, U.; Zhang, X.; Hellrung, B.; Haselbach, E.; Muller, P.-A.; Nau, W. M. *J. Am. Chem. Soc.* **2000**, *122*, 2027.

(30) (a) Heinze, J. *Angew. Chem., Int. Ed. Engl.* **1984**, *23*, 831. (b) Kiesele, H.; Heinze, J. In *Organic Electrochemistry*; Lund, H., Baizer, M. M., Eds.; Marcel Dekker: New York, 1991; p 331.

(31) (a) Bard, A. J.; Sadler, J. *J. Am. Chem. Soc.* **1968**, *90*, 1979. (b) Cheng, S.; Hawley, M. D. *J. Org. Chem.* **1985**, *50*, 3383.

(32) Anderson, L. B.; Broadhurst, M. J.; Paquette, L. A. *J. Am. Chem. Soc.* **1973**, *95*, 2198. For the reduced electron−electron repulsion in larger annulene dianions, see: Stevenson, G. R.; Forch, B. E. *J. Am. Chem. Soc.* **1980**, *102*, 5985.

(33) If the stereoelectronic differences between **1** (**2**) and **5** seem inadequate to explain the significantly different stability of the respective dianions, it should be recalled that comparable stereoelectronic differences in the structurally closely related series of dienes—pagodadiene ($d_{\pi\pi} \approx 2.8$ Å, $E_{1/2}$ = 0.66 V, E_{pc} = 1.20 V, ΔE = 0.54 V)/bishomododecahedradiene ($d_{\pi\pi} \approx 3.0$ Å, $E_{1/2}$ = 0.84 V, E_{pc} = 1.67 V)/secododecahedradiene ($d_{\pi\pi}$-(av) ≈ 3.0 Å, $E_{pc} \approx 0.8$ V)/1,16-dodecahedradiene ($d_{\pi\pi} \approx 3.5$ Å, $E_{pc} \approx 1.0$ V)—a second oxidation wave was observable only in the first two cases.[5,8]

(34) The delocalized structures presented in this work surfaced as the most favorable ones. Localized structures turned out to be either much higher in energy or even nonexistent. A detailed theoretical study of the $(N_2H_2)_2Li_{1/2}$ model systems and of the presented polycyclic radical anions and dianions, with and without inclusion of solvation effects, as well as the nature of the electronic transitions (Tables 1 and 2), will be subject of a forthcoming paper (Exner, K., manuscript in preparation).

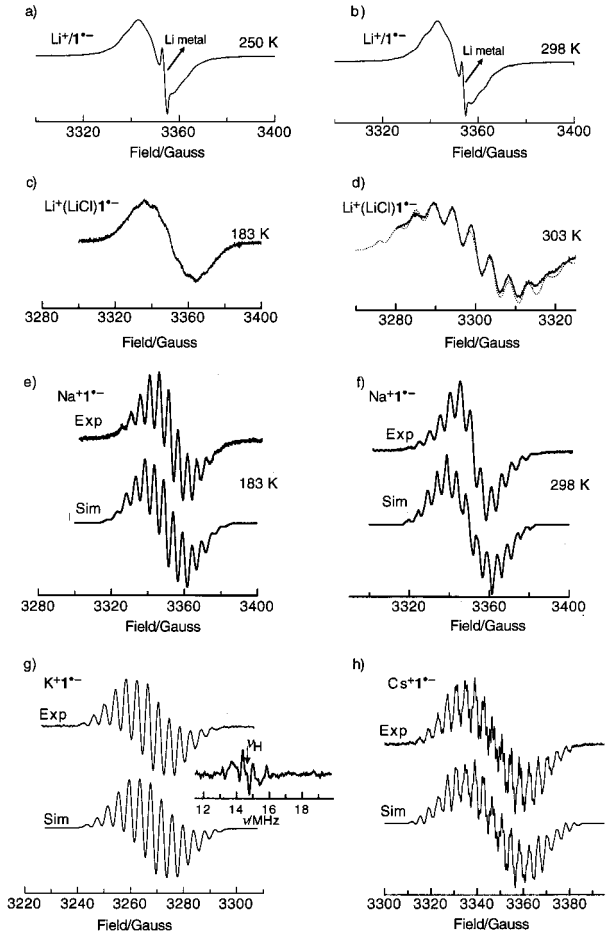

Figure 7. EPR spectra (THF) of $\mathbf{1}^{\bullet-}$ under various conditions: (a) $Li^+\mathbf{1}^{\bullet-}$, 250 K; the sharp central line stems from Li metal powder which could not be removed from the solution. (b) Same as (a), 298 K. (c) $Li^+(LiCl)\mathbf{1}^{\bullet-}$, generated upon addition of LiCl to the solution of $K^+\mathbf{1}^{\bullet-}$. (d) same as (c), 303 K, the dotted line represents the simulated spectrum. (e) $Na^+\mathbf{1}^{\bullet-}$, 183 K. (f) Same as (e), 298 K. (g) $K^+\mathbf{1}^{\bullet-}$, 233 K, the inset shows the ^{1}H ENDOR signals. (h) $Cs^+\mathbf{1}^{\bullet-}$, 233 K.

$K^+\mathbf{1}^{\bullet-}$ spectra proved temperature invariant in DME (203−303 K) as well as in THF (190−303 K); the ^{39}K hfc, assuming a comparable structure with $Cs^+\mathbf{1}^{\bullet-}$, should amount to 0.03 mT,[42] too small to be distinguished. In the $Cs^+\mathbf{1}^{\bullet-}$ spectra, the additional hfc of 0.318 mT is attributed to the ^{133}Cs nucleus ($I = {}^7/_2$).

For $K^+\mathbf{1}^{\bullet-}$, ENDOR and general TRIPLE experiments provided ^{1}H hfc's of +0.842, +0.098, +0.066, and −0.021 mT. The multiplicities of the ^{1}H and the ^{14}N hfc's (0.43 and 0.34 mT) were determined by simulation of the EPR spectra. [Note: Generally it is not always possible to detect ^{14}N hfc's by ENDOR spectroscopy; besides temperature, the viscosity of the solvent and the size of the ^{14}N hfc at various relaxation times play a decisive role (Plato, M.; Lubitz, W.; Moebius, K. *J. Phys. Chem.* **1981**, *85*, 1202).]

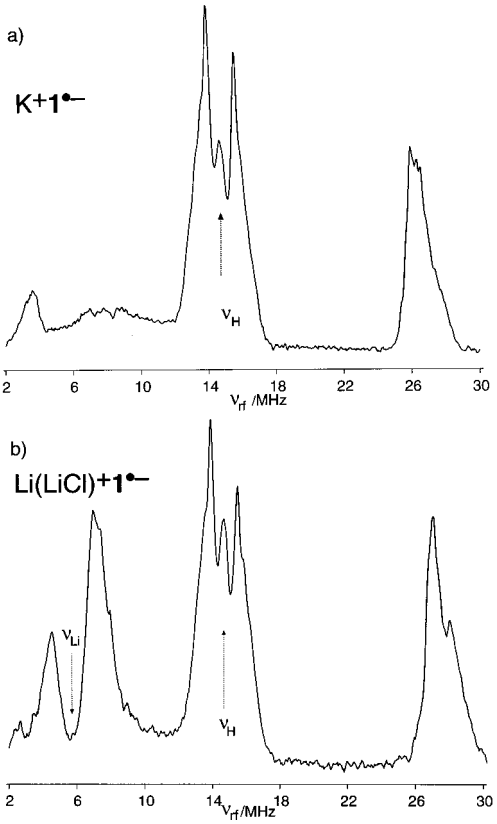

Figure 8. Davies-ENDOR spectra of $K^+\mathbf{1}^{\bullet-}$ (a) and $Li^+\mathbf{1}^{\bullet-}$ (b) (THF, 100 K, sum over 10 τ values).

CW ENDOR solution spectra, however, could not be obtained for the $Li^+\mathbf{1}^{\bullet-}$, $Li^+(LiCl)\mathbf{1}^{\bullet-}$, and $Na^+\mathbf{1}^{\bullet-}$ ion pairs due to saturation problems, and the CW spectra were not sufficiently resolved to determine ^{1}H and metal hfc's. To circumvent the saturation problem and to get some insight into the structures of the radical anions even in rigid media at low temperatures, various pulsed experiments such as Davies-ENDOR,[35] Mims-ENDOR,[36] three-pulse ESEEM (electron spin−echo envelope modulation),[37,38] and HYSCORE (hyperfine sublevel correlation)[39,40] were applied to $Li^+\mathbf{1}^{\bullet-}$, $Li^+(LiCl)\mathbf{1}^{\bullet-}$, $Na^+\mathbf{1}^{\bullet-}$, and $K^+\mathbf{1}^{\bullet-}$ at temperatures between 8 and 100 K.

Indeed, ^{1}H hfc's could be secured for all counterion−solvent combinations by ESEEM as well as by pulsed ENDOR. The spectra show that the ^{1}H hfc's are virtually independent of the counterion and the solvent. In the Davies-ENDOR spectra of $Li^+\mathbf{1}^{\bullet-}$ and $K^+\mathbf{1}^{\bullet-}$ (Figure 8), the signals belonging to the small ^{1}H hfc's with nearly isotropic shape are practically identical to those found by CW ENDOR in solution. A small anisotropic contribution with axial symmetry of the dominant ^{1}H hfc becomes distinct in the pulsed experiments ($A_\perp = 26.9$ MHz, $A_\parallel = 28.2$ MHz). Thus, it is ascertained that the $M^+\mathbf{1}^{\bullet-}$ structures are identical in the rigid and the fluid-solution states, and that the spin and the charge are delocalized over the entire 4N/5e system.

A benefit of the pulsed ENDOR and ESEEM measurements is the observation of $^7Li^+$ hfc's. With isotropic values of $a_{Li} = 2.3$ MHz (0.08 mT, THF) and $a_{Cs} = 0.32$ mT (THF) for $Cs^+\mathbf{1}^{\bullet-}$, the ratio of 10:2.5 is of the expected order of magnitude (10:1.7) and is another consequence of the closer association with the harder counterion. Splittings due to quadrupole interactions could not be observed.

The above results were verified by a HYSCORE experiment, a powerful two-dimensional method for measuring weak hy-

(35) Davies, E. R. *Phys. Lett. A* **1974**, *47*, 1.
(36) Mims, W. B. *Proc. R. Soc. A* **1965**, *283*, 452.
(37) Schweiger, A. *Angew. Chem., Int. Ed. Engl.* **1991**, *30*, 265.
(38) Mims, W. B. *Phys. Rev. B* **1972**, *5*, 2409.
(39) Hubrich, M.; Jeschke, G.; Schweiger, A. *J. Chem. Phys.* **1996**, *104*, 2172.
(40) Hoefer, P. *Appl. Magn. Reson.* **1996**, *11*, 375
(41) Bally, T.;. Sastry, G. N. *J. Phys. Chem.* **1997**, *201*, 77923.
(42) Relative metal hyperfine coupling constants (hfc's) for identical amounts of spin density in the metal *ns* orbitals: Q_M = l.74:3.84:1.00: 9.95. Nishiguchi, H.; Nakai, Y.; Nakamura, K.; Ishizu, K.; Deguchi, Y.; Takaki, H. *Mol. Phys.* **1965**, *9*, 153.

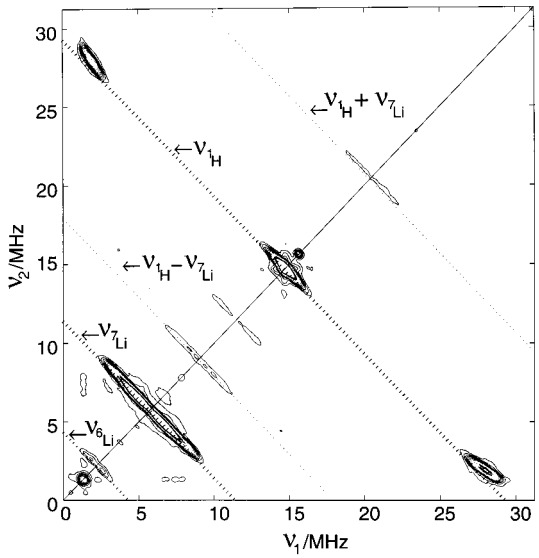

Figure 9. HYSCORE spectrum of $Li^+\mathbf{1}^{\bullet-}$ (sum over 3 τ values, (+,+) area).

perfine interactions in the solid state. Figure 9 shows a HYSCORE spectrum of $Li^+\mathbf{1}^{\bullet-}$, summed over seven different τ values. In these two-dimensional representations, the assignment of the hfc's is facilitated because the signals stemming from different nuclei are well separated. The diagonal represents the scale of the free nuclear frequencies of the individual nuclei. The hfc's are aligned along lines parallel to the antidiagonal. For example, the peaks belonging to the dominant ^{1}H hfc's of 23.6 MHz (0.84 mT) are positioned at ~27 MHz on both axes. The line connecting them bisects the diagonal at 15.8 MHz, the free ^{1}H frequency, ν_H. For ^{7}Li, the corresponding peaks are symmetrically spread around 5.8 MHz (because the hfc is small ($<2\nu_I$) and the quadrupole interaction of ^{7}Li can be neglected). The presence of the latter signals reflects the close association of Li^+ and $\mathbf{1}^{\bullet-}$, even at low temperatures, although ion-pairing is weakened by the increasing solvation power of the solvent. In addition, one observes the hfc of the ^{6}Li isotope ($\nu^{6}_{Li} = 2.2$ MHz) and combination frequencies between ^{1}H and ^{7}Li at $\nu^{1}_{H} + \nu^{7}_{Li}$ (20.4 MHz) and $\nu^{1}_{H} - \nu^{7}_{Li}$ (8.8 MHz). As for CW ENDOR, the ^{14}N hfc's, unambiguously secured by the simulation of the EPR spectra and by calculations, could not be observed by any of the pulsed resonance techniques.

For bisdiazenes **2**−**5**, well-defined and resolved EPR and ^{1}H ENDOR/general TRIPLE spectra were measured after one-electron reduction. In Figure 10, the EPR spectra of the ions $\mathbf{2}^{\bullet-}$−$\mathbf{5}^{\bullet-}$ with K^+ in THF as solvent are displayed. The simulations were accomplished with the help of ^{1}H hfc's from ENDOR measurements and ^{14}N hfc's shown in Figure 12. The ^{14}N hfc's are around 0.4 mT for all these radical anions, in very good conformity with $\mathbf{1}^{\bullet-}$. Moreover, the ion-pairing phenomena are also in accord with $\mathbf{1}^{\bullet-}$; e.g., the resolution of the spectrum of $Na^+\mathbf{2}^{\bullet-}$ improves at higher temperature. For $K^+\mathbf{5}^{\bullet-}$, even a ^{39}K hfc (0.071 mT) was detected. Note that $\mathbf{4}^{\bullet-}$ is the least persistent radical cation ($t_{1/2}$ for $K^+\mathbf{4}^{\bullet-} \approx 19$ min at 233 K), followed by $\mathbf{3}^{\bullet-}$ ($t_{1/2}$ for $K^+\mathbf{3}^{\bullet-} \approx 60$ min at 233 K). In contrast, $\mathbf{1}^{\bullet-}$, $\mathbf{2}^{\bullet-}$, and $\mathbf{5}^{\bullet-}$ were persistent for several hours under the same conditions. The persistence of the bisdiazene radical anions obviously reflects the absence (**1**, **2**, **5**) or presence (**3**, **4**) of acidic β protons and the distance between the two diazene moieties (d/d' in Figure 12). For **6** at temperatures as low as 203 K, no EPR signal was observed. In the case of **7** with $d =$ 4.887 Å, a transient EPR spectrum with a quintet pattern and a line distance of ~0.9 mT was observable at 200 K, typical for a localized monodiazene radical anion.

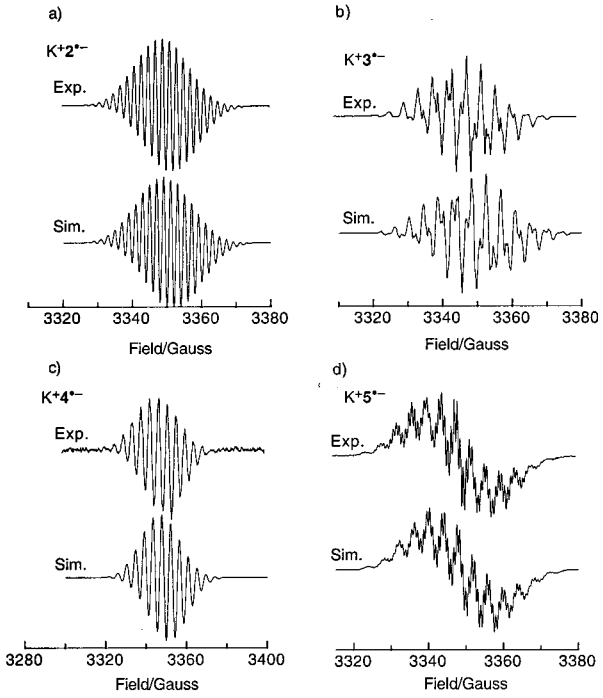

Figure 10. EPR spectra (THF) of (a) $K^+\mathbf{2}^{\bullet-}$, 233 K; (b) $K^+\mathbf{3}^{\bullet-}$, 233 K; (c) $K^+\mathbf{4}^{\bullet-}$, 233 K; (d) $K^+\mathbf{5}^{\bullet-}$, 233 K.

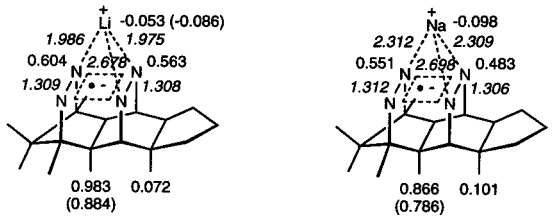

Figure 11. Calculated N═N/N═N distances, N═N bond lengths (UB3LYP/6-31G*, italics, Å), and hyperfine coupling constants (Davies-ENDOR, mT) for $Li^+\mathbf{1}^{\bullet-}$ and $Na^+\mathbf{1}^{\bullet-}$. Experimental data in brackets.

The assignment of the experimental ^{1}H hfc's in Figure 12 was based on spectral comparison and calculations. From a systematic check of HF and DFT methods in combination with various basis sets against the experimental data collected for $K^+\mathbf{1}^{\bullet-}$ (Table 5, Supporting Information), UB3LYP/6-31G*// UB3LYP/6-31G* emerged as the first choice.

An inherent deficiency of the B3LYP method is its propensity for inverse symmetry breaking, i.e., the inability to localize spin and/or charge.[41] Even for "distant" bisdiazene radical anions with $d \approx 5$ Å, such as $\mathbf{7}^{\bullet-}$, there is no tendency for spin localization. For the more reliable QCISD or CCSD methods, the present structures are by far too large. Yet, if the $H_4N_4^{\bullet-}$ model system is forced to geometrical restrictions (d, ω), as defined by the proximate bisdiazenes under study (**1**−**5**), preliminary CCSD(T)/D95+* calculations indicate the preference of delocalized C_{2v} over C_s structures with (beginning) localization. Thus, the application of the inexpensive B3LYP method to calculate geometries and hyperfine data is justified in these cases.

According to Table 4, the experimental ^{14}N hfc's are well reproduced, the 2(7)-H hfc is too small, and the 9(13)-H hfc is too large, presumably due to the neglect of the counterions in the calculations. For electrostatic reasons, the counterion should preferably be located above the 4N plane and should therefore

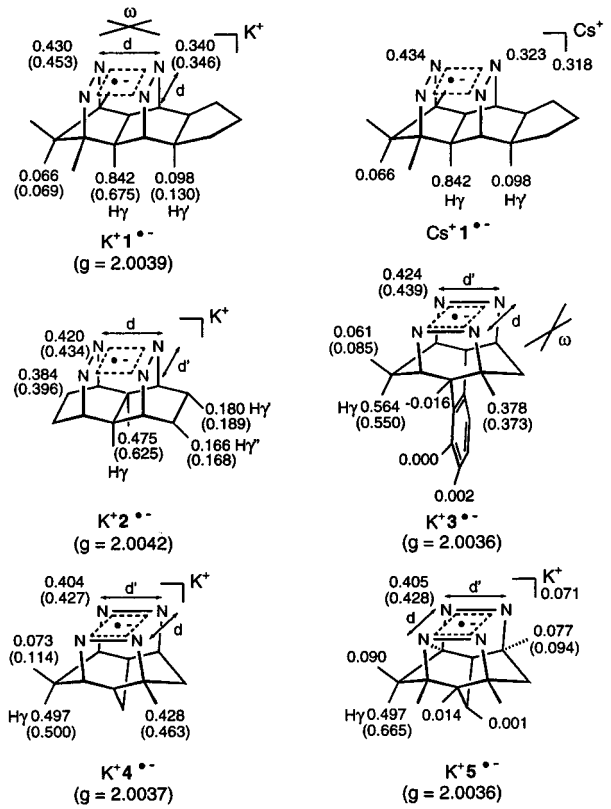

	1•−	2•−	3•−	4•−	5•−
d/d	2.69	2.69/2.75	2.85	2.96	2.83
d'/d'	1.31/1.30	1.35	1.29	1.29	1.29
ω	178.3	173.4	169.6	163.2	169.3
Δd	-0.14	-0.13/0.13	-0.17	-0.19	-0.26
Δω	+4.1	+4.6	+5.6	+6.9	+8.7

Figure 12. Experimental (ENDOR, spectrum simulation), calculated (brackets) ^{14}N and ^{1}H EPR coupling constants (mT, THF), and *g*-factors for K$^+$**1**$^{\bullet-}$−K$^+$**5**$^{\bullet-}$. Calculated (B3LYP/6-31G*) N═N/N═N distances (*d*, Å), N═N bond lengths (*d*′, Å), and interorbital angles (ω, deg) for the counterion-free anions **1**$^{\bullet-}$−**5**$^{\bullet-}$. Structural changes ($-\Delta d$, $+\Delta\omega$) vis-à-vis the neutrals **1**−**5**.

Table 4. Selected Calculated (UB3LYP/6-31G*) and Experimental Hyperfine Coupling Constants for **1**$^{\bullet-}$ and K$^+$**1**$^{\bullet-}$

	UB3LYP/6-31G*	exptl
N-4/N-5	0.453	0.430
N-14/N-15	0.346	0.340
1-H/8-H	−0.010	
2-H/7-H	0.675	0.842
9-H/13-H	0.130	0.098

concentrate the spin density between the two chromophores even further, causing even larger 2(7)-H and even smaller 9(13)-H hfc's. To test this hypothesis, structures and hfc's for Li$^+$**1**$^{\bullet-}$ and Na$^+$**1**$^{\bullet-}$ were calculated (neglecting the solvent, Figure 11). The metal ions are accommodated in a position practically symmetrical to the four N atoms, ∼1.3 and 2.3 Å, respectively, above the 4N plane. Compared with the data for the unpaired **1**$^{\bullet-}$, the N═N/N═N distances and N═N bond lengths are only marginally influenced, the γ-H hfc's are—more for the Li$^+$ than for the Na$^+$ pair—larger than the experimental ones (the ion-pairing effect is presumably overestimated as the coordinating solvent is neglected).[34] The negative sign for the ^{7}Li hfc is in line with the temperature dependence noted for the Li spectra.

Metal hfc's as measures of the ion pair association could be obtained by simulation of the EPR spectra for Cs$^+$**1**$^{\bullet-}$ (0.318 mT) and K$^+$**5**$^{\bullet-}$ (0.071 mT) and from pulsed EPR spectra of Li$^+$**1**$^{\bullet-}$ (0.086−0.091 mT) and Li/LiCl$^+$**1**$^{\bullet-}$ (0.086 mT). For ^{23}Na$^+$**1**$^{\bullet-}$, extrapolation of the ^{133}Cs$^+$**1**$^{\bullet-}$ hfc on the basis of the Q_M values[42]—with the assumption of equal ^{14}N and ^{1}H hfc's and equal spin population on the metal ions—leads to +0.123 mT, a value rather close to the 0.133 mT used for the simulation of the ^{23}Na$^+$**1**$^{\bullet-}$ spectrum (Figure 7).

What are the geometrical changes associated with the reductions **K** → **L**(**M**)? It is understood from the nodal properties of the LUMOs (cf. orbital MO3, Figure 1) that the N═N bonds (*d*′) should become longer, the N═N/N═N distances (*d*) shorter, and the angles ω larger. Calculated for the counterion-free anions, these changes (cf. Figures 5 and 12) are the smallest for the most proximate, most rigid bisdiazene **1** (→**1**$^{\bullet-}$, $\Delta d = -0.141$, $\Delta d' = 0.057$ Å, $\Delta\omega = 3.5°$), and the largest for the more "distant", more flexible **5** (→**5**$^{\bullet-}$, $\Delta d = -0.255$, $\Delta d' = 0.054$ Å, $\Delta\omega = 8.7°$).

In short, the EPR spectra uncover similarities with radical anions derived from the structurally related monodiazenes **M**−**O** (Figure 4) regarding the degree of ion association (increasing from soft to hard counterions) and the sign of the metal hfc's (changing from negative for Li$^+$ to positive for Na$^+$−Cs$^+$). As a distinctive difference, the ^{14}N hfc's for the ion pairs M$^+$**1**$^{\bullet-}$−M$^+$**5**$^{\bullet-}$ are only about half the size of the ^{14}N hfc's typically found for "localized" monodiazene radical anions **Q**$^{\bullet-}$−**S**$^{\bullet-}$ (0.8−0.9 mT) and confirm, within the hyperfine time scale, cyclic electron delocalization between the two N═N units. Additional support comes from the pulsed EPR measurements performed at temperatures as low as 8 K providing the same hyperfine data as established in fluid solution. Characteristic for the high concentration of spin density between the N═*N* units are the large hfc's for the central γ-H's, as opposed to the very small hfc's for the external γ'-H's (illustrated for counterion-free **1**$^{\bullet-}$ in Figure 17, Supporting Information). With $a_{H\gamma} = 0.38$ mT for monodiazene **8**, the large $a_{H\gamma}$ values are an additional strong argument against fast-equilibrating localized structures. Recall that the comparably large $a_{H\gamma} = 0.64$ mT for model diazene/ene **T** (Figure 4) had been related to N═N/C═C homoconjugative interaction. The increase of $a_{H\gamma}$ from K$^+$**1**$^{\bullet-}$ to Li$^+$**1**$^{\bullet-}$ is in line with stronger ion-pairing. Finally, EPR simulations using calculated hfc's of localized model systems for **1**$^{\bullet-}$ significantly deviate from the experimental spectra (Figure 18, Supporting Information).

In the case of M$^+$**1**$^{\bullet-}$ and M$^+$**2**$^{\bullet-}$, all alkali salts examined (Li$^+$, Na$^+$, K$^+$, Cs$^+$) proved thermally highly stable. Given the stability of the all-bridgehead-substituted K$^+$**5**$^{\bullet-}$, the relatively fast decomposition of K$^+$**4**$^{\bullet-}$ and K$^+$**6**$^{\bullet-}$ with rather close stereoelectronic properties (*d*,ω) is ascribed to faster tautomerization rather than to reduced electronic stabilization.

NMR Spectroscopic Measurements and Calculations

When the nature of the 4N/5e radical anions was established, σ-bishomoaromatic 4N/6e electronic structures for the corresponding dianions became highly probable. Still, even more than for the radical anions, the question was open to what degree the stability, and hence the observability, of the dianions, with their unusual concentration of six electrons in the plane and four *n*-electron pairs above the plane of the N_4 ring, would be affected by ion-pairing phenomena. Particularly for small, hard Li$^+$ counterions, the tetrazane-type configuration **L** in Figure 3, with pronounced covalent N···Li interaction minimizing charge repulsion, was considered a plausible alternative. Given small HOMO/LUMO gaps, the charge/charge repulsion could also be counterbalanced by changing from the singlet to the triplet state.

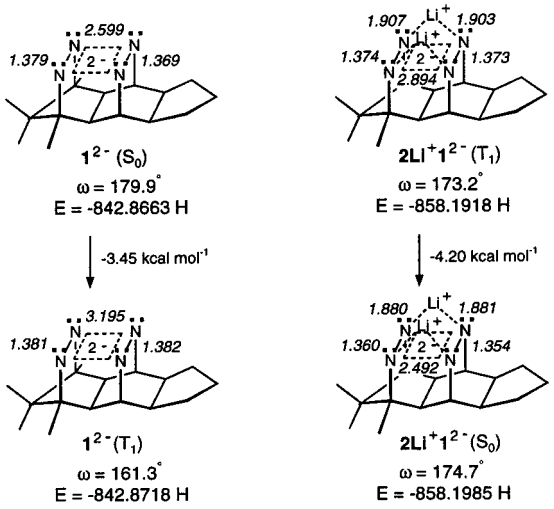

Figure 13. Calculated ((U)B3LYP/6-31G*) structures and energies (a.u.) for the S_0 and T_1 states of $\mathbf{1}^{2-}$ and $2Li^+\mathbf{1}^{2-}$.

This latter aspect was addressed by (U)B3LYP/6-31G* calculations for the counterion-free dianion $\mathbf{1}^{2-}$ as a representative example (Figure 13). In fact, the S_0 singlet state lies 3.5 kcal mol^{-1} above the T_1 triplet state, with rather long N═N/N═N distances (3.195 Å). In the S_0 state, with the addition of an electron into the A″ SOMO of the radical anion, the N═N/N═N distances (2.599 Å) become slightly shorter than in $\mathbf{1}^{\bullet-}$ ($\Delta d = -0.087$ Å), and the N═N bonds slightly longer ($\Delta d' =$ 0.063/0.051 Å). Yet, tight ion-pairing as in $2Li^+\mathbf{1}^{2-}$ places the singlet in the ground state. Neglecting the solvent, the metal ions occupy symmetry-equivalent positions ~1 Å above the 4N ring featuring (averaged) bond lengths of 1.357 and 2.492 Å. Orbital analyses support the cyclically delocalized 4N/6e configuration, which is electrostatically stabilized only by the counterions.

For the NMR study, again, only the bisdiazenes **1**, **2**, and **5** were used ([D_8]THF, in situ distilled from Na/K). After ~5−10 min of exposure to the metal, the now deeply red solutions (ca. 4×10^{-2} M) free of radical anions (no EPR signal) were transferred into NMR tubes under vacuum and sealed off. The generally well resolved ^{1}H and ^{13}C spectra were analyzed by NOE and heterodecoupling experiments (Figure 14).

After reduction of **1** with lithium the ^{1}H, ^{13}C, and ^{7}Li NMR spectra confirmed the retention of the C_s symmetry. As notable difference from the spectra of neutral **1**, the differentiation of the 16s/a-methyl groups due to the diamagnetic shielding by the neighboring N4═N5 double bond has vanished, the signals of the β-carbons and β-hydrogens (C(H)-1(8), C-3(6)) are diamagnetically shifted by 10.1 (1.96) and 15.6 ppm, and those of the central γ-carbons and γ-hydrogens (C(H)-2(7)) are paramagnetically shifted by 27.2 (1.09) ppm. In line with the symmetry of $2Li^+\mathbf{1}^{2-}$, only one ^{7}Li signal is registered (−2.73 ppm, half-width 0.07 ppm (233.2 MHz), external standard 0.1 M LiCl/H_2O).

The spectra of $2Na^+\mathbf{1}^{2-}$ were practically identical with those of $2Li^+\mathbf{1}^{2-}$, with comparable resolution and shifts. As already observed in the UV/vis study, the $2K^+\mathbf{1}^{2-}$ ion pair was not observable; the ^{1}H and ^{13}C spectra confirmed instead a uniform decomposition pathway (vide infra). For bisdiazene **2**, when reduced with Li, the NMR shift changes were comparable to those observed for **1**: diamagnetic shifts for the β-carbons (hydrogens) ($\Delta\delta(^1H) = -1.92/-2.06$ and $\Delta\delta(^{13}C)$ −8.6/−9.3), and paramagnetic shifts for the central γ-carbons (hydrogens) ($\Delta\delta(^1H) = +0.23$ and $\Delta\delta(^{13}C) = +23.6/+22.8$). The potassium salt $2K^+\mathbf{2}^{2-}$, in contrast to $2K^+\mathbf{1}^{2-}$, was stable but not soluble enough to provide a homogeneous solution; still, the poorly resolved spectra resembled those of $2Li^+\mathbf{2}^{2-}$. For $2Li^+\mathbf{5}^{2-}$, shifts that were analogous, but rather different in size, were noted ($\Delta\delta_{C-1(4,6,8)} = 19.4$, $\Delta\delta_{C-5(13)} = 20$ with respect to $2Li^+\mathbf{1}^{2-}$).

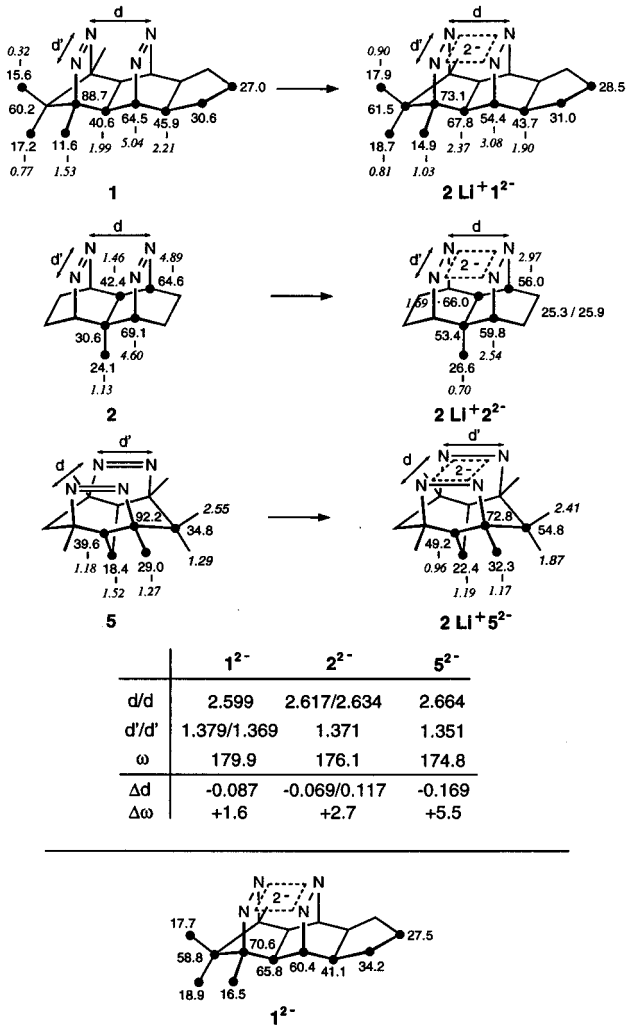

	1^{2-}	2^{2-}	5^{2-}
d/d	2.599	2.617/2.634	2.664
d'/d'	1.379/1.369	1.371	1.351
ω	179.9	176.1	174.8
Δd	-0.087	-0.069/0.117	-0.169
Δω	+1.6	+2.7	+5.5

Figure 14. ^{1}H (italics) and ^{13}C NMR shifts ([D_8]THF) for $2Li^+\mathbf{1}^{2-}$, $2Li^+\mathbf{2}^{2-}$, and $2Li^+\mathbf{5}^{2-}$. Calculated (B3LYP/6-31G*) N═N/N═N distances (*d*, Å), N═N bond lengths (*d*′, Å), interorbital angles (ω, deg), and changes ($-\Delta d$, $+\Delta\omega$) vis-à-vis the respective radical anions. Calculated ^{13}C shifts for counterion-free $\mathbf{1}^{2-}$.

What is the role of the counterions? The PMSE-GIAO/B3LYP/6-31G*-calculated[43] ^{13}C spectrum well matched the experimental one. Deviations no larger than 6 ppm suggest only slight perturbations of the 4N/6e electronic structures even by the Li^+ counterion. What are the geometrical changes (Δd, $\Delta\omega$) associated with the second reduction? The comparison of the data calculated for counterion-free dianions (Figure 14) with that of the radical anions (Figure 12) attests to minor additional shortening of the N═N/N═N distances (Δd at most ≈ 0.12 Å) and consequently slightly better in-plane orientation of the p-orbitals ($\Delta\omega$ up to 3°).

With the HOMO for $\mathbf{1}^{2-}$ (Figure 15, almost identical with that of $2Li^+\mathbf{1}^{2-}$), the essential NMR information is summarized: Cyclic six-electron delocalization with high charge concentration between the N═N units!

(43) Chemical shieldings were calculated using the GIAO method. Conversion to chemical shifts was done by comparison with σ (^{13}C, TMS). To account for solvent effects, a constant shift was applied in order to minimize the simple error of the calculated shifts, cf. ref 13.

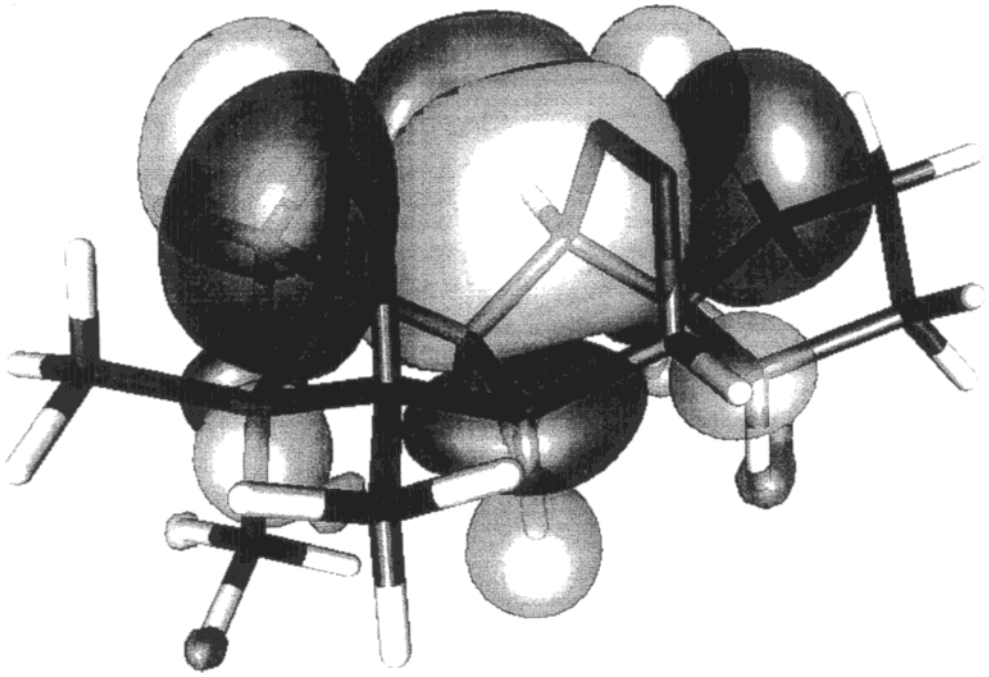

Figure 15. Calculated HOMO of counterion-free $\mathbf{1}^{2-}$ (B3LYP/6-31G*; the surfaces correspond to an electron density of ± 0.02 e bohr^{-3}).

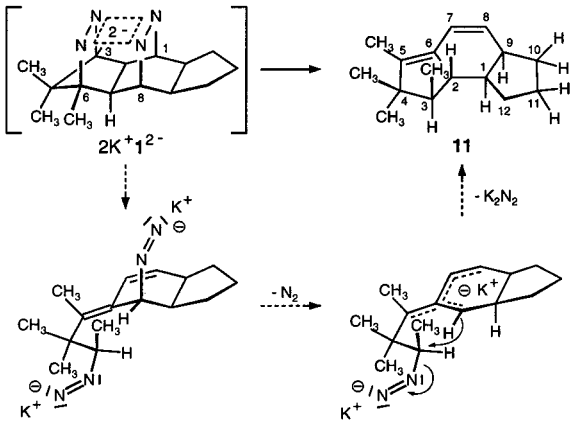

Figure 16. Decay of the weakly associated $2K^+\mathbf{1}^{2-}$ ion pair.

The importance of the degree of ion-pairing for the observability of the 4N/6e dianions has been experienced in the reduction of $K^+\mathbf{1}^{\bullet-}$ (the green color directly changed into dirty brown). As was learned from the structure of the nearly quantitatively formed product, the tricyclic $C_{16}H_{24}$ hydrocarbon **11** (the stereochemistry was established by extensive NOE and decoupling experiments), this molecular corset responds to the enormous charge−charge repulsion in the weakly associated $2K^+\mathbf{1}^{2-}$ by skeletal cleavage, ultimately with extrusion of the two N═N units (as N_2 and $2K^+N_2^{2-}$?) (Figure 16).

Concluding Remarks

Cyclic electron delocalization (σ-bishomoaromaticity) in the plane made up of four centers—known in 4C/3(2)e cations of type **A**(**B**) (Figure 2) but not in the analogous 4C/6(5)e anions **E**(**F**) (Figure 3)[44,45]—has now been realized in 4N rings. By a gratifyingly productive interplay of experiment (UV/vis, CV, EPR, NMR) and theory (DFT), the nature of the green radical anions and the red dianions generated by the reduction of particularly preoriented bisdiazenes (**1**−**5**, N═N distances up to ~3.2 Å, interorbital angles as small as ~155°) as cyclically delocalized, bishomoconjugated 4N/5e radical anions and σ-bishomoaromatic 4N/6e dianions is firmly established. Particularly remarkable are the short homoconjugated N···N bonds and the nearly perfect in-plane orientation of the bond-forming orbitals for the radical anions (2.7−3.0 Å, $\omega = 179-163°$) and for the dianions (2.6−2.7 Å, $\omega = 180-175°$). The degree of ion-pairing, differences in thermodynamic stabilization due to the gradually changing stereoelectronic situations ($d_{\pi\pi}$, ω), and (not the least) the skeletal-specific kinetic protection make up for the lifetime of these ions ranging from months to seconds at room temperature (the dianions are relatively weak bases, THF as solvent is not deprotonated). The electrochemical measurements allow a first, qualitative estimate of the thermodynamic stabilization which the 4N/5e radical anions enjoy due to the five-electron in-plane delocalization. For the 4N/6e dianions, a more quantitative assessment of the "σ-bishomoaromaticity" of the resulting energetic contribution and magnetic properties ("ring current") is expected from calculational analyses.[34,46]

Competition experiments with the 4N/6(5) anions, the preparation of ^{15}N-enriched substrates (^{15}N chemical shifts, coupling constants), quenching experiments,[47] the potential of the dianions as ligands,[48] crystal structure analyses of radical anions and dianions, the construction of tetra-N-cage structures[49] for which the sp*x*,sp*x* in-plane delocalization in the form of the

(44) The similarly small cyclobutadiene (π) dianion is calculated to sacrifice the square aromatic structure for a puckered nonaromatic one for the sake of reduced electron−electron repulsion:[1c] (a) Hess, B. A.; Ewig, C. S.; Schaad, L. J. *J. Org. Chem.* **1985**, *50*, 5869. (b) Glukhovtsev, M. N.; Simkin, B. Ya.; Minkin, V. I. *Zh. Org. Khim.* **1987**, *23*, 1317. Extended π-delocalization makes $C_4O_4^{2-}$ moderately aromatic: (c) Ito, M.; West, R. *J. Am. Chem. Soc.* **1963**, *85*, 2580. (d) Schleyer, P. v. R.; Najafian, K.; Kiran, B.; Jiao, H. *J. Org. Chem.* **2000**, *65*, 426. Recently, an X-ray structure of a cyclobutadiene dianion dilithium salt was published: Sekiguchi, A.; Matsuo, T.; Watanabe, H. *J. Am. Chem. Soc.* **2000**, *122*, 5652. For a brief review touching the interplay of electronic stabilization and Coulombic effects in π-conjugated anions: Benshafrut, R.; Shabtai, E.; Rabinovitz, M.; Scott, L. T. *Eur. J. Org. Chem.* **2000**, 1091.

(45) For our early attempts in the ballpark of 5C/6e anions,[1a] see: Eberbach, W.; Prinzbach, H. *Chem. Ber.* **1969**, *102*, 4162.

(46) Schleyer, P. v. R.; Jiao, H. *Pure Appl. Chem.* **1996**, *28*, 209.

(47) In exploratory experiments, 1,4-homoconjugative addition of HOAc to $2Li^+\mathbf{2}^{2-}$ delivered the respective tetrazane.[14]

(48) For example: Bach, I.; Pörschke, K.-R.; Proft, B.; Goddard, R.; Kopiske, C.; Krüger, C.; Rufinska, A.; Seevogel, K. *J. Am. Chem. Soc.* **1997**, *119*, 3773.

tetrahomoconjugate 4N/7(6)e (di)cations depending on the skeletal mobility ("in−out isomerism") would have to compete with the tetrahedral[50] 4N/7(6)e, and the well-established linear 2N/3(2)e bonding motifs[11,51] are topics of active investigation.[52] It is appropriate to remark that the return for the enormous investment into synthesis[10,53] has already been additionally rewarded by the more recent demonstration of in-plane delocalization in 4N/3(2)e cations (better represented as cubically delocalized 4N4O/11(10)e cations?),[54,55] in 4N radical cations, in 4N cations,[56] and in 4N anions.[56,57] Very recently, an alternative access to the 4N/6(5) anions has been opened, involving the oxidation of the "anions" generated by metalation of the bishydrazines derived inter alia from the bisdiazenes utilized in the present reduction study (Figure 5).[58]

Even though the existence of four-centered, anionic 4N homoconjugation (σ-bishomoaromaticity), as the central theme of this paper, is bound to exceptional, and in every respect expensive, molecular corsets, the 4N/5e radical anions and 4N/6e dianions presented are more than just "curiosities"—particularly the dianions, with their extreme concentration of charge, stand as impressive manifestations for the power of enforced proximity, disclosing novel, intricate facets of chemical bonding.

Experimental Section

The CV curves were recorded in carefully purified and dried argon-purged THF with tetrabutylammonium hexafluorophosphate as supporting electrolyte (Philips model PM 8271 X−Y recorder). For the higher scan rates, a model PS0 8100 imk transcient recorder was used. A three-electron configuration was employed throughout. The working electrode was a Pt disk (diameter 1 mm) sealed in soft glass, the counter electrode a Pt wire coiled around the glass mantle of the working electrode, and the reference electrode an Ag wire on which AgCl had been deposited electrochemically, immersed in the electrolyte solution. Potentials were calibrated against the formal potentials of ferrocene (+0.35 V vs Ag/AgCl) and cobaltocene (−0.94 V vs Ag/AgCl). The measurements were performed with a Jaissle potentiostat IMP88 and a PAR 175 programmer. For the preparation of the radical anions, see refs 19−22. ESR and optical spectra were recorded simultaneously on a Varian E9 spectrometer with an optical cavity to which a TIDAS diode array spectrometer (J&M, Aalen, Germany) was attached. CW-EPR and CW-ENDOR spectra were recorded with a Bruker ESP 300 spectrometer, and Mims- and Davies-ENDOR three-pulse ESEEM and HYSCORE experiments were conducted with a Bruker ESP 380 spectrometer. All manipulations were carried out under an argon atmosphere. The quantum chemical calculations were performed with Gaussian 94 (revision E.2),[26a] and the DF calculations with Becke's three-parameter hybrid functional[26b] using the correlation functional developed by Lee, Yang, and Parr.[26c]

3,4,4,5-Tetramethyltricyclo[7.3.0.0^{2,6}]dodeca-5,7-diene (11). The brownish, homogeneous THF solution resulting from the reduction of **1** (136 mg, 0.50 mmol) with potassium (one reaction product, TLC) was quenched with water/pentane. After standard workup with very careful removal of the pentane, the colorless, highly volatile oil (ca. 70 mg, the yield is reduced by loss during concentration) was found to be pure **11**. ^{1}H NMR ([D$_8$]THF, THF = 1.73, 400 MHz): δ = 6.23 [ddd, J = 0.4 Hz, $J_{7,9}$ = 1.8 Hz, $J_{7,8}$ = 9.9 Hz, 7-H], 5.81 [dd, $J_{8,9}$ = 4.8 Hz, $J_{8,7}$ = 9.9 Hz, 8-H], 2.37 [dddd, $J_{9,7}$ = 1.8 Hz, $J_{9,8}$ = 4.8 Hz, $J_{9,10\alpha}$ = $J_{9,1}$ = 6.7 Hz, $J_{9,10\beta}$ = 12.0 Hz, 9-H], 1.92 [m, 12-H], 1.91 [m, $J_{2,5-Me}$ = 2.1 Hz, $J_{2,3}$ = 9.0 Hz, 2-H], 1.87 [m, 10-Hα], 1.82 [m, 1-H], 1.78 [m, 11-Hβ], 1.73 [m, 12-H], 1.63 [d, $J_{5-Me,2}$ = 2.1 Hz, 5-Me], 1.55 [m, 11-Hα], 1.41 [dq, $J_{3,3-Me}$ = 6.6 Hz, $J_{3,2}$ = 9.0 Hz, 3-H], 1.24 [m, 10-H$_a$], 1.07 [d, $J_{3-Me,3}$ = 6.6 Hz, 3-Me], 0.96 [s, 4-Meα], 0.76 [s, 4-Meβ]. ^{13}C NMR ([D$_8$]THF, THF = 25.30): δ = 140.1 (C-6), 133.1 (C-5), 131.5 (C-8), 121.7 (C-7), 52.9 (C-3), 50.2 (C-2), 44.8 (C-1), 44.1 (C-9), 33.6 (C-10), 32.2 (C-12), 25.9 (4-Me$_\alpha$), 25.6 (C-11), 19.6 (4-Me$_\beta$), 14.1 (3-Me), 9.7 (5-Me), 48.9 (C-4). MS (EI): *m*/*z* (relative intensity) 216 [M$^+$] (15), 201 [M$^+$ − Me] (100), 159 (19), 145 (40), 91 (30). $C_{16}H_{24}$ (216.4).

Acknowledgment. The Freiburg groups thanks the BASF AG, the Deutsche Forschungsgemeinschaft, the VW Foundation, and the Fonds der Chemischen Industrie for financial support, B. Geiser, V. Perron and H. Moschallski for technical assistance, Dr. D. Hunkler and Dr. J. Wörth for NMR and MS spectral measurements, and Dr. L. Knothe for discussions and help with the manuscript.

Supporting Information Available: Table 5, listing calculated (**1**$^{\bullet-}$) and experimental (K$^+$**1**$^{\bullet-}$) hyperfine coupling constants; Figure 17, showing the calculated spin density distribution for counterion-free **1**$^{\bullet-}$ (UB3LYP/6-31G*); and Figure 18, showing simulations of the EPR spectra of counterion-free delocalized and "localized" **1**$^{\bullet-}$ (PDF). This material is available free of charge via the Internet at http://pubs.acs.org.

JA0014943

(49) (a) Heitzmann, M.; Yang, F.; Kegel, M.; Prinzbach, H., manuscript in preparation. (b) Nelsen, S. F.; Buschek, J. M. *J. Am. Chem. Soc.* **1974**, *96*, 6424.

(50) Bremer, M.; Schleyer, P.v. R.; Scholz, K.; Kausch, M.; Schindler, M. *Angew. Chem., Int. Ed. Engl.* **1987**, *26*, 761.

(51) (a) Gerson, F.; Gescheidt, G.; Knöbel, J.; Martin, W. B., Jr.; Neumann, L.; Vogel, E. *J. Am. Chem. Soc.* **1992**, *114*, 7107. (b) Alder, R. W. *Tetrahedron* **1990**, *46*, 683−713. (c) Alder, R. W. *Acc. Chem. Res.* **1983**, *16*, 321. (d) Kirste, B.; Alder, R. W.; Sessions, R. B.; Bock, M.; Kurreck, H.; Nelsen, S. F. *J. Am. Chem. Soc.* **1985**, *107*, 2635.

(52) Vögtle, M. Dissertation, University of Freiburg, 2000.

(53) Exner, K.; Fischer, G.; Lugan, M.; Fritz, H.; Hunkler, D.; Keller, M.; Knothe, L.; Prinzbach, H. *Eur. J. Org. Chem.* **2000**, 787.

(54) Exner, K.; Prinzbach, H.; Gescheidt, G.; Grossmann, B.; Heinze, J. *J. Am. Chem. Soc.* **1999**, *121*, 1964.

(55) (a) C.f. the 10e in-plane delocalized systems: Sagl, D. J.; Martin, J. C. *J. Am. Chem. Soc.* **1988**, *110*, 5827. (b) Kobayashi, K.; Takahashi, O.; Namatame, K.; Kikuchi, O.; Furukawa, N. *Chem. Lett.* **1998**, 515. (c) Fokin, A. A.; Jiao, H.; Schleyer, P. v. R. *J. Am. Chem. Soc.* **1998**, *120*, 9364. (d) McEwen, A. B.; Schleyer, P. v. R. *J. Org. Chem. Soc.* **1986**, *51*, 4357.

(56) Exner, K.; Grossmann, B.; Gescheidt, G.; Heinze, J.; Keller, M.; Bally, T.; Bednarek, P.; Prinzbach, H. *Angew. Chem., Int. Ed.* **2000**, *112*, 1514. For "σ-allyl cations", see: (a) Paquette, L. A.; Usui, S. *Tetrahedron Lett.* **1999**, *40*, 3499. (b) Baldridge, K. K.; Leahy, J.; Siegel, J. S. *Tetrahedron Lett.* **1999**, *40*, 3503 and references cited therein.

(57) Exner, K.; Vögtle, M.; Prinzbach, H., to be published.

(58) Geier, J. Diplomarbeit; Kegel, M. Dissertation, University of Freiburg, 2000.